International Food Research Journal 31(5): 1107 - 1119 (October 2024)
Journal homepage: *http://www.ifrj.upm.edu.my*

Pasting and viscoelastic properties of starches isolated from tropical fruits

[1]Martínez-Ortiz, M. A., [1,3]Balois-Morales, R., [1,3]Bello-Lara, J. E.,
[2]Chavarría-Hernández, N. and [2]*Rodríguez-Hernández, A. I.

[1]Doctorado en Ciencias Biológico Agropecuarias, Universidad Autónoma de Nayarit, Carretera Tepic-Compostela km 9, Xalisco, Nayarit, C. P. 63780, México
[2]Cuerpo Académico de Biotecnología Agroalimentaria, Instituto de Ciencias Agropecuarias, Universidad Autónoma del Estado de Hidalgo, Av. Universidad km 1, Exhacienda de Aquetzalpa, Tulancingo de Bravo, Hidalgo, C.P. 43600, México
[3]Unidad de Tecnología de Alimentos - Secretaría de Investigación y Posgrado, Universidad Autónoma de Nayarit, Ciudad de la Cultura, Colonia Centro, Tepic, Nayarit, C.P. 63000, México

Article history

Received:
13 October 2023
Received in revised form:
10 July 2024
Accepted:
12 July 2024

Keywords

mango,
soursop,
banana,
fruit-derived starch,
starch viscoelasticity

Abstract

The exploration of new starch sources has increased due to the demand to develop green materials. In this sense, diverse polysaccharides, including starch, can be isolated from fruits due to their significant postharvest loss in many countries with vast fruit biodiversity. The present work examined the chemical composition, morphology, and rheological properties of starches isolated from tropical fruits in Mexico, namely: (1) stenospermocarpic mango (*Mangifera indica* L.) 'Ataulfo', which is considered a postharvest loss due to its small size and no commercial value; (2) 'Pera' banana (*Musa* ABB), a low commercial value fruit; and (3) soursop (*Annona muricata* L.), a highly perishable fruit. The research concerning the morphological and rheological properties of those starches is scarce to date. The starches presented amylose contents ranging between 24.7 and 29.4% (w/w), congruent with the amylose content in most normal native starches. During pasting, the viscosities of the 7% fruit starch suspensions were higher than those of the normal corn starch (reference). Mango and soursop starches are rapid-swelling starches; their pasting temperatures were 66.3 and 69.5°C, respectively. Banana starch showed the highest peak viscosity value (0.89 Pa s), and soursop starch pastes exhibited the lowest retrogradation tendency (setback viscosity = 0.168 Pa s). After cooling, the starch pastes exhibited soft gel-like viscoelastic behaviour. Accordingly, the rheological characterisation of the pastes and gels of the isolated starches allows us to propose them as new starches for diverse food and biotechnological applications.

DOI
https://doi.org/10.47836/ifrj.31.5.03

Introduction

Starch is the principal storage polysaccharide of plants, consisting of different proportions of amylose and amylopectin. Some physicochemical properties of starches, such as swelling, pasting, and gelation capacity, are essential in industrial processes (Singh *et al.*, 2003). Thus, the structural and functional diversities of starch make them suitable for industrial applications such as foods, pharmaceuticals, paper processing, and biodegradable packaging. Starch as an agro-sourced polymer has become well-accepted due to its wide availability in nature, low cost, and total biodegradability. The exploration of new starches from non-conventional sources has recently increased due to the demand for green materials, bioplastics for food packaging, and innovative starch-based products. In this sense, low-valued fruits have become increasingly used to isolate polysaccharides due to their significant postharvest loss in many countries with vast fruit biodiversity.

Mango (*Mangifera indica* L.) is a popular tropical fruit, widely grown and cultivated in many tropical regions worldwide, with India, China, Brazil, and Mexico being the major mango producers (FAO, 2023). The 'Ataulfo' mango is native to Chiapas State, Mexico, and well accepted for its sensory attributes in the international and national markets. Until 2021, Mexico was the world's largest exporter of mangoes (FAO, 2023). However, mangoes are affected by a phenomenon known as fruit stenospermocarpic,

*Corresponding author.
Email: inesr@uaeh.edu.mx

yielding small-sized mangoes (< 118 g), and considered a postharvest loss (Hernández-Guerrero *et al.*, 2020).

Another tropical fruit with high demand in global markets is banana, which comprises several species or hybrids in the genus *Musa* of the family Musaceae (Marta *et al.*, 2022). Cultivation faces enormous challenges: plant diseases, low prices, and the need to improve the practices for sustainable production. Bananas or plantains are climacteric fruits, which, once cut from the tree, begin an accelerated maturation process that causes significant postharvest losses, so technological alternatives must be sought to diversify their utilisation. In its green or immature state, banana has up to 70% starch by dry basis, an amount that is comparable to that present in some cereals, legumes, and tubers traditionally used for starch isolation (Agama-Acevedo *et al*., 2015).

Soursop (*Annona muricata* L.) is a fruit native to Latin America, and very perishable; its shelf life is limited to five days at room temperature when harvested at physiological maturity (Coêlho de Lima and Alves, 2011). Furthermore, soursop is prone to damage caused by phytopathogenic fungi during postharvest due to fruit handling system, storage conditions, transport, and commercialisation, causing postharvest losses of up to 40% in developing countries (González-Ruíz *et al*., 2021).

Commercially, starches are obtained mainly from corn, wheat, rice, and tubers or roots such as potato and tapioca; nonetheless, efforts have been carried out to find alternative starch sources to take advantage of the vastly available bioresources worldwide. In this sense, several investigations have been carried out to characterise starches from mango and banana. Espinosa-Solis *et al*. (2009) isolated and characterised starch from ‘Tommy Atkins’ mango and ‘Macho’ banana (*Musa paradisiaca* L.). The authors reported that the fruit starches presented lower pasting temperatures, but higher peak and final viscosities than maize starch. On the other hand, Lagunes-Delgado *et al*. (2022) characterised the starch from unripe mango of Haden and Palmer cultivars, which presented C-type crystalline pattern and subtle differences in gelatinisation temperatures, 74.5 and 78.4°C, respectively, and were categorised as rapid swelling starches. Starches from soursop have been scarcely studied. Nwokocha and Williams (2009) isolated starch from soursop; the starch presented an amylose content close to 20%, spherical granules with an average size of less than 10 µm, and its functional behaviour was similar to waxy corn starch.

Therefore, the present work aimed to analyse the physicochemical, morphological, pasting, and rheological properties of starches extracted from low-valued fruits, namely 'Pera' banana (*Musa* ABB), stenospermocarpic 'Ataulfo' mango, and soursop, which have been little addressed in studies about the extraction of biomacromolecules of industrial interest. The findings of the present work would provide a theoretical basis for further food and biotechnological applications of these novel native starches.

Materials and methods

Materials

Stenospermocarpic 'Ataulfo' mango, soursop, and 'Pera' banana were used for starch isolation (Figure 1). The different fruits were harvested at physiological maturity, and obtained from Atonalisco, Compostela, and San Blas in Nayarit, Mexico, respectively. Corn starch (Sigma Aldrich, S-4126) was used as a reference (amylose = 28.30 ± 0.90%, protein = 0.13 ± 0.02%). Amylose (Sigma Aldrich A0512), amylopectin (Sigma Aldrich A8515), and dimethyl sulfoxide (Sigma Aldrich 276855) were used for starch chemical characterisation. Distilled water was used throughout.

Starch isolation

Starch isolation was carried out by wet grinding using an industrial blender with citric acid (food additive grade) as an antioxidant (0.3%, w/w) (Flores-Gorosquera *et al.*, 2004), then filtered through meshes of 85, 425, 150, and 75 µm. The recovered liquid phase was allowed to settle until starch precipitation. Afterwards, it was washed with distilled water, and separated by centrifugation at 1,537 *g* for 5 min (Hermle Z216 MK, Germany). Finally, the starch was dried in a convection oven at 40°C for 24 h. The resulting starch was weighed and stored in sealed airtight containers until use.

Amylose, amylopectin, and protein determination

The amylose content was determined by the method described by Hoover and Ratnayake (2001). Briefly, 20 mg of starch were dissolved in 8 mL of 90% dimethyl sulfoxide, and the mixture was heated in a water bath at 85°C for 30 min with intermittent mixing on a heating plate. The mixture was diluted to

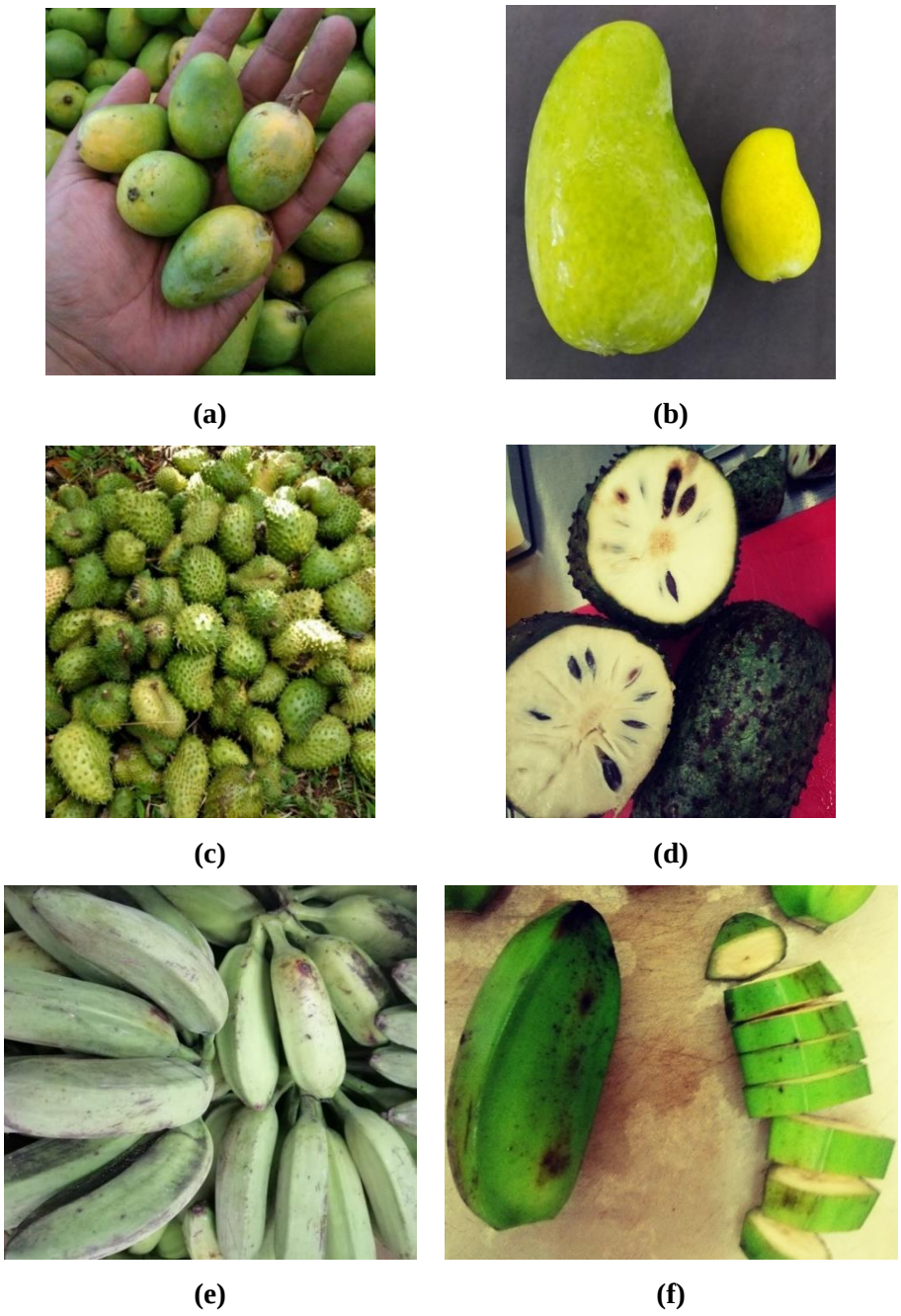

Figure 1. Tropical fruits used to isolate starches; **(a)** stenospermocarpic mango 'Ataulfo' (*Mangifera indica* L.); **(b)** stenospermocarpic mango 'Ataulfo' (right) and normal 'Ataulfo' mango (left); **(c)** soursop (*Annona muricata* L.); **(d)** soursop cross-section; and **(e)** and **(f)** 'Pera' banana (*Musa* ABB).

25 mL with distilled water in a volumetric flask. Next, 1 mL aliquot was mixed with 40 mL of distilled water and 5 mL of I_2/KI, and adjusted to a final volume of 50 mL with distilled water. It was then left to react for 15 min at room temperature, and absorbance readings were taken at 600 nm against a reagent blank, using a nano-spectrophotometer (BioTek, Synergy HT 7091000, GEN v2.01.14 software). A standard curve of amylose/amylopectin was made with amylose solution at different concentrations of 0, 10, 15, 20, 25, and 30%. The results were expressed as a percentage of amylose (% amylose). The difference in the amylose content determined the amylopectin content. The crude protein content of isolated starches was determined following the official AOAC methodology using a nitrogen conversion factor of 6.25, and the results were expressed on a dry basis. All determinations were performed in triplicate.

Fourier-transform infrared spectroscopy (FT-IR)

The chemical structure of starches was confirmed through Fourier-transform infrared (FTIR) spectroscopy using an FTIR spectrometer (Cary 630, Agilent Technologies Inc. USA) equipped with a single bounce diamond ATR accessory. Spectra were obtained by co-adding 32 scans at a resolution of 4 cm^{-1} in the spectral region of 4,000 - 600 cm^{-1}. Data were collected and analysed using Resolutions Pro® software (Agilent Technologies Inc. USA).

Scanning electron microscopy (SEM)

The morphology of starches was analysed using a scanning electron microscope (mini-SEM SNE-3200M, South Korea). The starches were placed on a double-adhered conductive tape, coated with a 60 nm gold layer, and analysed at a voltage of 20 kV.

Light microscopy of starch swelling

The morphology of the isolated starch granules was observed during the pasting process, following the methodology described by Rodríguez-Hernández (2004). Briefly, 7% starch-water suspensions were placed in a rheometer equipped with a starch cell (AR2000, TA Instruments, USA), and a heating ramp (4°C/min) was carried out with constant stirring (16.8 rad/s) from 50 to 90°C. During heating, 200-µL aliquots were taken at temperatures 25, 65, 75, 85, and 90°C. After the aliquots were diluted to 1:10 with distilled water, they were shaken and placed in a cold-water bath (12°C) to avoid subsequent swelling of the granules. Then, 10 µL of the resulting dilution were taken and mixed with 10 µL of Lugol's solution (0.0025 M I_2/0.0065 M KI). A drop of the dilution was placed on a slide, and observed under bright field microscopy on a Nikon Eclipse 80i (Tokyo, Japan) microscope equipped with a camera using the NCB11 filter. The time between sampling and observation was less than 10 min.

Pasting properties

The viscosity profiles of starch suspensions were analysed using an AR2000 rheometer (TA Instruments, USA) equipped with a starch pasting cell geometry (SPC, TA Instruments), which consisted of a cell jacket, an impeller with blades at the bottom for sample mixing, and aluminium cup with locking cover. Slurry (7% starch) was loaded into the starch cell, and preheated at 50°C for 1 min. Then, a pre-shear (90 rad/s, 20 s) was carried out to avoid starch sedimentation. Next, the thermo-mechanical program was executed as follows: the starch suspension was heated from 50 to 90°C (4°C/min), held for 10 min, and then cooled to 50°C (4°C/min). The rotation speed was maintained at 16.8 rad/s throughout the program. All starches were tested in triplicate. Pasting parameters: pasting temperature, peak viscosity, hold viscosity, breakdown viscosity, final viscosity, and setback viscosity were then determined (BeMiller, 2019).

Viscoelastic properties of starch gels

Small-amplitude oscillatory strain tests were performed in a strain-controlled rheometer (ARES-G2, TA Instruments, USA) equipped with a plate-plate fixture (sandblasted steel, diameter = 40 mm, Δh = 1 mm) and a solvent trap. Starch pastes (7%, w/w), recently prepared in a starch pasting cell as previously described in the previous section, were poured rapidly on the preheated plate-plate fixture (85°C) immediately after the holding time at 90°C, then were cooled to 25°C (5°C/min), and a ten min-period of resting of the sample at 25°C was done. Afterwards, a frequency sweep from 10^2 to 10^{-2} rad/s was carried out at constant strain and 25°C. The region of linear viscoelasticity was determined previously using recently prepared starch pastes (Rodríguez-Hernández *et al*., 2006).

Statistical analysis

Results were reported as mean ± standard deviation. An analysis of variance (ANOVA) and a mean comparison using Tukey's test ($p < 0.05$) were performed using SigmaPlot® software version 14.5 (Systat Software Inc.).

Results and discussion

Chemical analysis

Mango starch presented the lowest amounts of protein, 0.32 ± 0.13% (w/w) dry basis, while soursop and banana starches showed similar values, 0.55 ± 0.05 and 0.61 ± 0.02% (w/w) dry basis, respectively. The protein content in the starches may be residual endosperm storage protein stuck to the surface of granules, or residual enzymes entrapped within the granule (BeMiller, 2019). It has been reported that proteins in starch granules had a noticeable impact on the pasting properties of rice starches (0.27 to 0.76% protein content); the proteins associated with starch granules promoted the structural stability of the starch system, and those located in the channel of starch

granules protected them from shearing during gelatinisation (Zhan *et al.*, 2020).

On the other hand, the isolated starches presented amylose contents lower than 30% (w/w), which agreed with the amounts of amylose present in most normal native starches (20 - 32%) (Singh *et al.*, 2003; Chen *et al.*, 2019); the amylose contents were 29.40 ± 0.40, 24.67 ± 0.60, and 28.00 ± 1.06% for mango, soursop, and banana, respectively. Similar values (31.1%) have been reported for starches isolated from the 'Tommy Atkins' mango (Espinosa-Solis *et al.*, 2009), and starches isolated from unripe mangoes of Haden and Palmer cultivars (33.8 and 22.5%, respectively) (Lagunes-Delgado *et al.*, 2022). Banana starch has been more widely studied; starches isolated from various banana clones, including *Musa* AAB, 'White Manzano', 'Dwarf Cavendish', 'Valery', 'Enano', 'Morado', 'Macho', and 'Terra' presented amylose contents of 19.3 to 37.88% (Marta *et al.*, 2022). Amylose contents of 19.31 to 35% have been reported for starch isolated from soursop (Nwokocha and Williams, 2009).

FT-IR spectroscopy

FT-IR spectroscopy was used to identify the functional groups in the dry starch samples, and confirm the starch structure. Figure 2 shows the FT-IR spectra of native starches isolated from mango, soursop, and banana, and commercial corn starch was used as a reference. The prominent bands in the IR spectra were observed close to 3,309, 2,900, 1,635, 1,335, 1,148, 1,075, 993, 928, and 859 cm^{-1}. Those bands were present in all the samples, including the reference one. The broadband in the region 3,000 - 3,600 cm^{-1} is attributed to the O–H stretching of glucopyranose rings in starch; C–CH_2-C asymmetric stretching vibrations occur at 2,891 - 2,925 cm^{-1}. The band at ~1,640 cm^{-1} is associated with the moisture

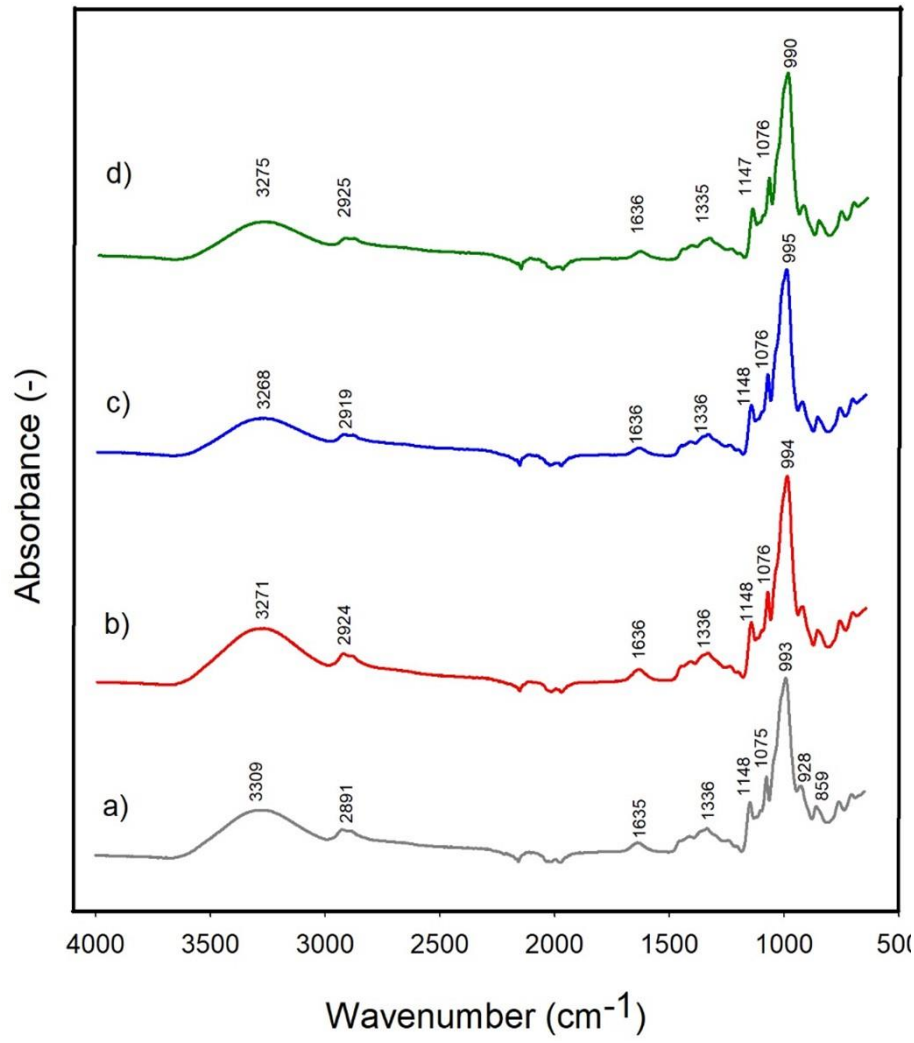

Figure 2. FTIR spectra for starches from: **(a)** corn (reference); **(b)** stenospermocarpic mango 'Ataulfo' (*Mangifera indica* L.); **(c)** soursop (*Annona muricata* L.); and **(d)** 'Pera' banana (*Musa* ABB).

content of the samples, and it arises from the vibrations of adsorbed water molecules in the non-crystalline region (Xiong *et al.*, 2017). The bands between 1,200 and 1,700 cm^{-1} are related to minor components in the starch samples (protein and lipid residues) (Warren *et al.*, 2016). The characteristic peaks of starch are in the region of 800 – 1,300 cm^{-1}, which are sensitive to the conformational and crystalline order of starch (Xiong *et al.*, 2017). FT-IR spectrum of corn starch (reference starch) (Figure 3a) shows five characteristic peaks at 1,148, 1,075, 993, 928, and 859 cm^{-1}, which are assigned to C–O, C–C, and C–O–H stretching vibrations, and C–O–H bending vibrations of pyranose rings (Xiong *et al.*, 2017). These characteristic bands were also observed in the native starches from mango, soursop, and banana (Figures 2b, 2c, and 2d), confirming that the isolated starches had the same basic structure in the dry state like the native corn starch. The intense band at 991 - 995 cm^{-1} is assigned to the intermolecular bonding of OH groups in the C6 position, which is exclusively observed in native starches because of their hydrophilicity (Govindaraju *et al.*, 2022). In addition, that intense band near 1,000 cm^{-1} is attributed to the amylose and amylopectin in starch samples (Ma *et al.*, 2021; Govindaraju *et al.*, 2022).

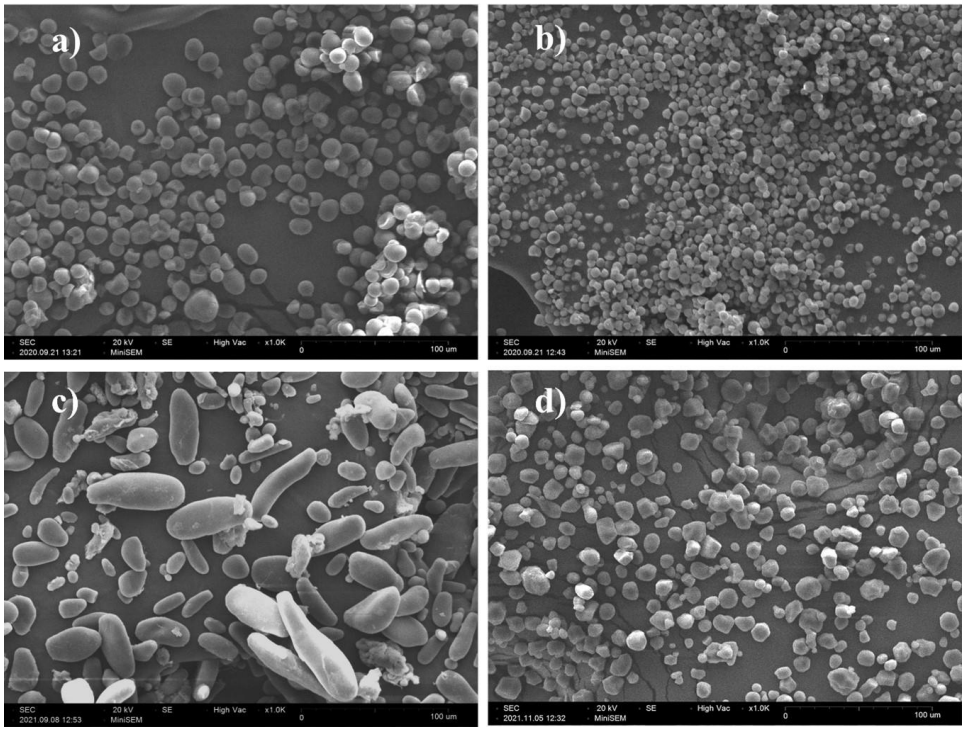

Figure 3. Scanning electron microscopy of starches from: **(a)** stenospermocarpic mango 'Ataulfo' (*Mangifera indica* L.); **(b)** soursop (*Annona muricata* L.); **(c)** 'Pera' banana (*Musa* ABB); and **(d)** corn starch (S-4126, Sigma-Aldrich). Magnification: 1,000×; bar scale = 100 µm.

Morphology of starch granules

Scanning electron microscopy (SEM) revealed the shapes, surface morphology, and size of starch granules. The photographs of the starch granules from mango, soursop, and banana are shown in Figure 3. Starch from stenospermocarpic mango showed smooth surface granules having round, semispherical, or dome-shaped granules, with diameters ranging between 6.3 and 18.6 µm. The starch from soursop showed small granules; they exhibited irregular, spherical, and truncated shapes with diameters between 5.6 and 9.6 µm. Banana starch granules had irregular, elongated, and lenticular shapes, with diameters between 12.7 and 28.8 µm, and lengths of 10.2 to 59.9 µm. The photograph of granules corresponding to corn starch (reference starch) is presented in Figure 3d, which exhibits polygonal shapes with diameters lower than 20 µm, which in turn agrees with data reported for large corn starch granules (15 to 20 µm) (Singh *et al.*, 2003).

The morphology of the fruit starch granules agreed with similar studies; diverse SEM photographs of starches isolated from mango described the granules as round and semispherical, with some truncated ones (Lagunes-Delgado *et al.*, 2022). The granule size of banana starch is more

prominent than other starches, and depends on the clone and the ripening state. Micrographs of the starch from various banana clones have shown irregular, elongated, and ellipsoidal granules ranging from 20 to 60 µm (Marta *et al*., 2022). Although there are few reports on soursop starch, the morphology of its granules is described as spherical, truncated, and irregular, with granule sizes ranging from 2.49 to 7.68 µm (Nwokocha and Williams, 2009). The starch source primarily determines the morphology of the starch granules. The shape and size of the granule directly influence the pasting process and the rheological properties of the pastes and gels (Singh *et al*., 2003; Rodríguez-Hernández *et al*., 2006).

Pasting properties

The photomicrographs of the aqueous slurry of starch granules during the gelatinisation process are displayed in Figure 4a. Lugol's iodine solution stained granules dark blue due to the formation of amylose-iodine complexes. Photomicrographs exhibited shapes and relative sizes consistent with those observed in SEM (Figure 3). As the starch slurry is heated and sheared, the starch granules swell due to water absorbed in the amorphous regions, and the melting of the crystalline regions within starch granules. Gelatinisation occurs when an irreversible loss of order is carried out; amylose is leached into the continuous medium, and the granules swell. The complete swelling process is recognised by presenting a population of swollen granules, granule fragments (granule ghosts and other remnants) suspended in a solution of mostly amylose (BeMiller, 2019). Gelatinisation is followed by pasting, which is the formation of a viscous starch paste *via* further granule swelling, additional amylose leaching, and disruption of the granules due to the continued heating of starch under shearing in excess of water. Understanding the gelatinisation and pasting processes of native starches allows us to better predict their functional properties.

The gelatinisation process and pasting profile of the slurry of starches are commonly examined by measuring the viscosity of the starch suspension while heating and cooling under testing conditions (shear, heating rate, holding time, and cooling rate). The resultant pasting curve yields essential parameters, such as the pasting temperature, peak, setback, and final viscosities. The pasting profiles of starches examined in the present work are shown in Figure 4b. The profiles display the changes in the viscosity of 7% starch suspensions under continuous stirring (16.8 rad/s) as a function of time and temperature.

The fruit starches had amylopectin contents similar to the corn starch used as a reference. It is widely accepted that amylopectin content and chain length distribution are crucial factors for the swelling behaviour of starches. Low molecular weight amylopectin with long branched chains facilitates the formation of the amylose-lipid complex, which restricts the swelling of granules, and elevating the pasting temperature. On the other hand, amylose influences the packaging of amylopectin into crystallites, and their organisation within the granules, which determines starch gelatinisation (Cornejo-Ramírez *et al*., 2018; BeMiller, 2019). Thus, the differences observed in pasting profiles in Figure 4b are mainly due to the composition and structural organisation of the starch granules (*i.e*., granule size, crystalline structure, and minor components).

The pasting temperature indicates the temperature at which the viscosity of the starch dispersion begins to increase during the initial heating phase. Mango and soursop starches showed lower pasting temperatures than banana and corn starches. The pasting curve of the fruit starches showed an abrupt change in the viscosity, while corn starch showed a smaller slope on its viscosity profile during the first 11 min of the heating phase; after that, a sharp increase was observed. The increasing viscosity correlated to the increase in the effective volume fraction of swollen granules (Gutiérrez-Córtez *et al*., 2021), and the extent of their integrity. Therefore, the starch concentration (7%, w/w) used in the present work allowed a progressive swelling of the granules until reaching a maximum viscosity value (peak viscosity) detected at temperatures higher than 85°C (except for mango starch). Soursop starch showed two peaks in its viscosity curve, one near 84°C, and the second during the holding time at 90°C, where the maximum viscosity was detected.

Based on the morphological changes observed by optical microscopy (Figure 4a), mango starch showed leached material from 65 to 90°C, and the presence of swollen granules, damaged granules, and amylose in the continuous medium was evident from 75°C. These granules were probably more sensitive to heat and shear stress, yielding a paste with more significant amounts of disrupted granules (Figure 4a). For soursop starch, granules swelled at 65°C without

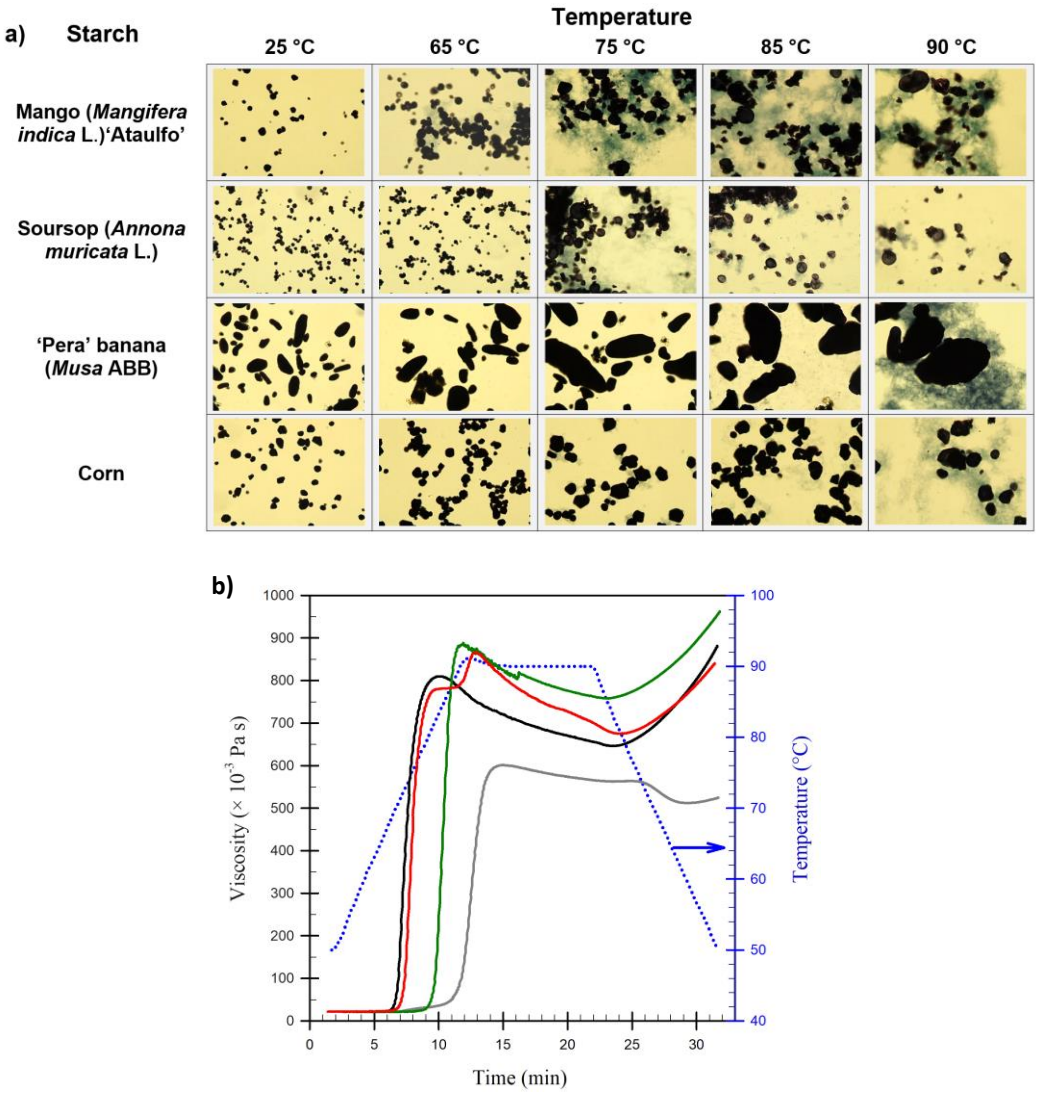

Figure 4. (a) Morphological structure of starch granules during pasting. Magnification: 400×. **(b)** Pasting profiles of starches: corn (reference) (grey line); stenospermocarpic mango (*Mangifera indica* L.) 'Ataulfo' (black line); soursop (*Annona muricata* L.) (red line); and 'Pera' banana (*Musa* ABB) (green line).

apparent damaged granules or leached amylose. At 75°C, more swollen granules and leached amylose were observed, and more damaged granules were detected at higher temperatures. A heterogeneous mixture of swollen granules with different sizes embedded in a continuous phase was observed. That complex system could generate an additional increase in the viscosity after 85°C due to the contribution of the viscosity of the continuous phase (amylose dispersed), and the presence of smaller swollen granules. Nwokocha and Williams (2009) reported that soursop starch starts its gelatinisation at 65.7°C and completes at 75.3°C, which agreed with the morphological changes observed in the present work during soursop starch pasting.

Banana starch presented higher resistance to thermo-mechanical treatment. The swelling continued without the amylose leaching or the apparent damage to its granules up to 75°C. This agreed with Chávez-Salazar *et al.* (2017), who found gelatinisation temperatures between 70 and 80°C, and that the high thermal resistance of the banana starch granules was related to the heterogeneity of their size and the internal arrangement of the double helices of amylopectin chains. The pasting properties of banana starch varied depending on the cultivar, but pasting temperatures ranging between 70 and 83°C have been reported (Marta *et al.*, 2022). Based on the pasting profile (Figure 4b), all starches isolated from fruits displayed higher viscosities than the corn starch used

as a reference, which showed a progressive swelling of its granules as temperature increased, and the leaching of amylose was evident from 75°C. That was consistent with the gelatinisation temperature range reported for normal corn starch (*i.e.*, 75-80°C) (BeMiller, 2019). The development of higher viscosity in fruit starches can be related to the internal structure of the granules, which allows them to swell more than cereal starches. Similar findings were reported for starches isolated from 'Macho' banana and 'Tommy Atkins' mango, whose final paste viscosities (0.351 and 0.361 Pa s, respectively) were higher than barley and corn cereal starches (0.027 and 0.123 Pa s, respectively) (Espinosa-Solis *et al*., 2009). The maximum viscosity attained during the heating process (peak viscosity) ranged between 801 and 888 mPa s for fruit starches, while corn starch showed a value of 602 mPa s (Table 1). Banana starch showed the highest peak viscosity, attributable to the size and swelling behaviour of the starch granule (Figure 4a). During the holding time at 90°C, all fruit starches decreased in viscosity due to more granules disintegrating, while corn starch showed a lower decrease.

Table 1. Pasting properties of starches.

Starch	Pasting temperature (°C)	Peak viscosity ($\times 10^{-3}$ Pa s)	Breakdown viscosity ($\times 10^{-3}$ Pa s)	Setback viscosity ($\times 10^{-3}$ Pa s)	Final viscosity ($\times 10^{-3}$ Pa s)
Stenospermocarpic 'Ataulfo' mango (*Mangifera indica* L.)	66.3 ± 0.1	801.6 ± 6.9	642.0 ± 7.0	232.1 ± 3.2	871.4 ± 10
Soursop (*Annona muricata* L.)	69.5 ± 0.2	867.7 ± 9.6	675.1 ± 4.1	167.7 ± 4.3	842.1 ± 8.5
'Pera' Banana (*Musa* ABB)	72.9 ± 0.5	887.8 ± 5.5	756.7 ± 1.4	203.0 ± 2.0	959.4 ± 3.6
Corn	72.0 ± 0.3	601.8 ± 0.2	509.4 ± 2.8	12.2 ± 0.3	521.6 ± 3.1

Values are mean ± standard deviation of three replicates, $n = 3$.

Breakdown viscosity is a measure of susceptibility to the disintegration of the cooked starch (Shevkani *et al*., 2011). Banana starch showed the highest breakdown viscosity resulting from its higher swelling behaviour, as shown in Figure 4a, and the heterogeneity of the size granules. On the other hand, corn starch showed the lowest breakdown viscosity. During the cooling phase, amylose molecules re-associate to form a network, yielding gels or more viscous pastes. This process is called setback, which is determined as the difference between the final viscosity and the trough viscosity, and it is important to determine the starch gel stability because it indicates the retrogradation tendency of starch granules upon the cooling of cooked pastes (Deng *et al.*, 2020). Among isolated starches, soursop starch exhibited the lowest retrogradation tendency. These results indicated that soursop starch had good freeze-thaw stability, and potential use in frozen foods.

Viscoelastic properties of starch gels

Figure 5a shows the frequency sweeps for 7% starch gels formed upon cooling the cooked pastes. The storage moduli, G' (ω), were higher than the loss moduli, G" (ω), throughout the examined frequency range. The gelation process resulted in G' (ω) independent of frequency ($G' \propto \omega^{0.001\text{-}0.054}$) in all cases. Moreover, G" (ω) of fruit starches exhibited a notable frequency dependence ($G'' \propto \omega^{0.219\text{-}0.289}$) with a trend to crossover the G' (ω) curve at high frequencies. An elastic plateau was only observed in corn starch at $\omega < 1$ rad/s (Figure 5a). The mechanical spectra are typical of slightly structured systems with no strong interactions between macromolecules apart from topological entanglements (Doublier and Llamas, 2005). The liquid-like character prevails when starch gels are sheared at high frequencies, while their elastic-like behaviour is evidenced at low frequencies or longer observation times. The same viscoelastic behaviour in starch gels has been reported before (Rodríguez-Hernández *et al.*, 2006; Savary *et al*., 2008). Starch gels have been described as composites or filled-matrix composites where the filler is a complex mixture of intact, partially swollen, and disrupted granules, and the matrix is the amylose network forming the continuous phase. The rheological behaviour of starch gels results from the

organisation of amylose chains to form a network in which the filler is embedded. That process occurs during the cooling and subsequent resting stage of the pastes. Thus, the viscoelastic properties of the amylose network formed, the volume fraction of swollen granules, their deformability, and the adhesion characteristics (inter-particle bonding) between granules and the continuous medium determine the viscoelastic properties of starch gels. The amylose content and its chain extension are also associated with starch gel viscoelasticity; starches with higher amylose contents produce firm gels. Based on Figure 5a, corn starch produced the firmest gel, with G'(ω) values close to 1,000 Pa; mango and banana starches showed G'(ω) values between 200 and 450 Pa, and soursop starch gels yielded the lowest G'(ω) values (90 - 130 Pa). Soursop starch had the lowest values of amylose content, while the rest of the starches analysed did not present a significant difference in that content. Therefore, the differences observed in G'(ω) can be attributed to the molar sizes of amylose chains, amylopectin molecules in solution, and the strengthening effect of the amylose network due to the presence of swollen granules that remained after pasting. Previous work showed that the extent of disintegration of the granules has a strong effect on the elastic character of starch gels. The pasting conditions, where more granule swelling and less granular breakdown are generated, give rise to more elastic starch gels (Savary *et al.*, 2008).

Figure 5b displays the loss tangent values (tan δ = G'(ω)/ G''(ω)), which, unlike those of corn starch, have a significant frequency dependence, yielding values from 0.02 to 0.28. That behaviour is characteristic of soft gels or weak viscoelastic gels, and it has been reported in works concerning gels of native starches (Núñez-Santiago *et al*., 2004; Xiong *et al*., 2017; Xu *et al*., 2021). For the fruit-derived starches, the combination of parameters such as the volume fraction of swollen granules, their extent of disruption after the pasting process, the deformability of swollen granules, and the elasticity of continuous phase generated less rigid gels than those observed for corn starch, even when the pastes of this last starch were less viscous. Normal cereal starches are known to retain rigid and swollen granules, and develop strong gels (Ai and Jane, 2018). Therefore, those rigid granules contribute less to the paste viscosity, but act as fillers in the amylose network during starch gelation, improving the solid-like behaviour.

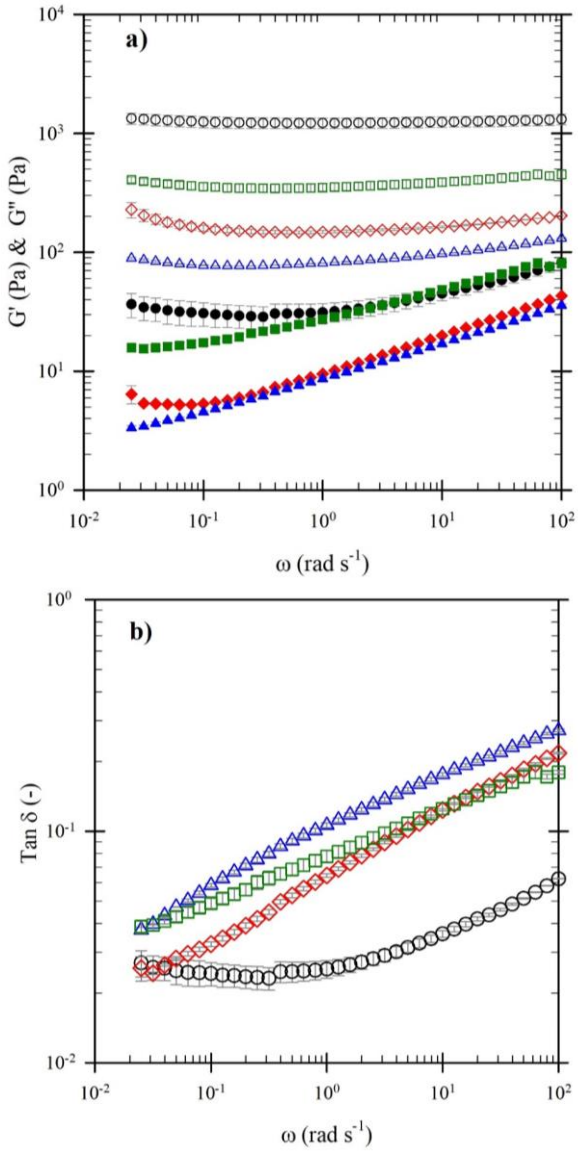

Figure 5. (a) Frequency sweeps at 25°C and **(b)** loss tangent (tan δ) of: corn starch (●) (γ = 2%); stenospermocarpic mango (*Mangifera indica* L.) 'Ataulfo' (♦) (γ = 4.5%); soursop (*Annona muricata* L.) (▲) (γ = 3.5%); and 'Pera' banana (*Musa* ABB) (■) (γ = 4.5%). G': hollow symbols; G'': filled symbols.

Conclusion

Starches isolated from 'Pera' banana (*Musa* ABB), stenospermocarpic mango (*Mangifera indica* L.) 'Ataulfo', and soursop (*Annona muricata* L.) yielded amylose contents between 24.7 and 29.4%. The fruit starches displayed higher viscosities during pasting than the normal corn starch used as a reference. Mango and soursop starches can be categorised as rapid swelling starches; they showed low pasting temperatures, and their granules were

very sensitive to thermomechanical treatment. Banana starch had the most prominent granules; a heterogeneous population of swollen and disrupted granules was observed at the end of its pasting, and it showed the highest peak viscosity value. After cooling, 7% starch pastes showed viscoelastic properties of soft gels or slightly structured systems. The combination of parameters such as the size of granules, their extent of disruption after the pasting process, the deformability of swollen granules, and the continuous phase's elasticity generated soft gels with G'(ω) values ranged between 450 and 90 Pa. The chemical and rheological properties of the starches from those low-valued fruits provide valuable insights for further study and applications as stabiliser, and gelling and thickening agents for developing green materials, bioplastics for food packaging, and innovative starch-based products for the food industry, where consumers usually demand for clean-label products.

Acknowledgement

Martínez-Ortiz M. A. acknowledges the Consejo Nacional de Humanidades, Ciencias y Tecnologías (CONAHCYT) (approval no.: CVU 621813) for the PhD scholarship. The present work was financially supported by CONAHCYT (grant nos.: 316558; 230138) and the Secretary of Agriculture, Livestock, Rural Development, Fisheries, and Food (SAGARPA; grant no.: 266891). The authors are grateful to Alejandra Torres Blancas for revising the English language of the manuscript.

References

Agama-Acevedo, E., Nuñez-Santiago, M. C., Álvarez-Ramírez, J. and Bello-Pérez, L. A. 2015. Physicochemical, digestibility and structural characteristics of starch isolated from banana cultivars. Carbohydrate Polymers 124: 17-24.

Ai, Y. and Jane, J.-l. 2018. Chapter 3 - Understanding starch structure and functionality. In Sjöö, M. and Nilsson, L. (eds). Starch in Food (2nd ed), p. 151-178. United States: Woodhead Publishing.

BeMiller, J. N. 2019. Starches: Molecular and granular structures and properties. In BeMiller, J. N. (ed). Carbohydrate Chemistry for Food Scientists (3rd ed), p. 159-189. United States: AACC International Press.

Chávez-Salazar, A., Bello-Pérez, L. A., Agama-Acevedo, E., Castellanos-Galeano, F. J., Álvarez-Barreto, C. I. and Pacheco-Vargas, G. 2017. Isolation and partial characterization of starch from banana cultivars grown in Colombia. International Journal of Biological Macromolecules 98: 240-246.

Chen, J., Chen, L., Xie, F. and Li, X. 2019. Starch. In Chen, J., Chen, L., Xie, F. and Li, X. (eds). Drug Delivery Applications of Starch Biopolymer Derivatives, p. 29-40. Singapore: Springer.

Coêlho de Lima, M. A. and Alves, R. E. 2011. Soursop (*Annona muricata* L.). In Yahia, E. M. (ed). Postharvest Biology and Technology of Tropical and Subtropical Fruits, p. 363-392. United States: Woodhead Publishing.

Cornejo-Ramírez, Y. I., Martínez-Cruz, O., Del Toro-Sánchez, C. L., Wong-Corral, F. J., Borboa-Flores, J. and Cinco-Moroyoqui, F. J. 2018. The structural characteristics of starches and their functional properties. CyTA - Journal of Food 16(1): 1003-1017.

Deng, M., Reddy, C. K. and Xu, B. 2020. Morphological, physico-chemical and functional properties of underutilized starches in China. International Journal of Biological Macromolecules 158: 648-655.

Doublier, J. L. and Llamas, G. 2005. A rheological description of amylose-amylopectin mixtures. In Dickinson, E. and Walstra, P. (eds). Food Colloids and Polymers, p. 138-146. United States: Woodhead Publishing.

Espinosa-Solis, V., Jay-Lin, J. and Bello-Pérez, L. A. 2009. Physicochemical characteristics of starches from unripe fruits of mango and banana. Starch 61(5): 291-299.

Flores-Gorosquera, E., García-Suárez, F. J., Flores-Huicochea, E., Núñez-Santiago, M. C., González-Soto, R. A. and Bello-Pérez, L. A. 2004. Yield of starch extraction from plantain (*Musa paradisiaca*) - Pilot plant study. Acta Científica Venezolana 55(1): 86-90.

Food and Agriculture Organization (FAO). 2023. Major tropical fruits: Market review 2022. Rome: FAO.

González-Ruíz, A. V., Palomino-Hermosillo, Y. A., Balois-Morales, R., Ochoa-Jiménez, V. A., Casas-Junco, P. P., López-Guzmán, G. G., ... and Bautista-Rosales, P. U. 2021. Pathogenic fungi associated with soursop fruits (*Annona muricata* L.) during postharvest in Nayarit, Mexico. Horticulturae 7(11): 471.

Govindaraju, I., Zhuo, G.-Y., Chakraborty, I., Melanthota, S. K., Mal, S. S., Sarmah, B., … and Mazumder, N. 2022. Investigation of structural and physico-chemical properties of rice starch with varied amylose content: A combined microscopy, spectroscopy, and thermal study. Food Hydrocolloids 122: 107093.

Gutiérrez-Córtez, E., Hernadez-Becerra, E., Londono-Restrepo, S. M. and Rodriguez-Garcia, M. E. 2021. Physicochemical characterization of Amaranth starch insulated by mechanical separations. International Journal of Biological Macromolecules 177: 430-436.

Hernández-Guerrero, S. E., Balois-Morales, R., Palomino-Hermosillo, Y. A., López-Guzmán, G. G., Berumen-Varela, G., Bautista-Rosales, P. U. and Alejo-Santiago, G. 2020. Novel edible coating of starch-based stenospermocarpic mango prolongs the shelf life of mango "Ataulfo" fruit. Journal of Food Quality 2020: 1320357.

Hoover, R. and Ratnayake, W. S. 2001. Determination of total amylose content of starch. Current Protocols in Food Analytical Chemistry 1: E2.3.1-E2.3.5.

Lagunes-Delgado, C., Agama-Acevedo, E., Patiño-Rodríguez, O., Martinez, M. M. and Bello-Pérez, L. A. 2022. Recovery of mango starch from unripe mango juice. LWT - Food Science and Technology 153: 112514.

Ma, Y., Zhang, W., Pan, Y., Ali, B., Xu, D. and Xu, X. 2021. Physicochemical, crystalline characterization and digestibility of wheat starch under superheated steam treatment. Food Hydrocolloids 118: 106720.

Marta, H., Cahyana, Y., Djali, M. and Pramafisi, G. 2022. The properties, modification, and application of banana starch. Polymers 14(15): 3092.

Núñez-Santiago, M. C., Bello-Pérez, L. A. and Tecante, A. 2004. Swelling-solubility characteristics, granule size distribution and rheological behavior of banana (*Musa paradisiaca*) starch. Carbohydrate Polymers 56(1): 65-75.

Nwokocha, L. M. and Williams, P. A. 2009. New starches: Physicochemical properties of sweetsop (*Annona squamosa*) and soursop (*Annona muricata*) starches. Carbohydrate Polymers 78(3): 462-468.

Rodríguez-Hernández, A. I. 2004. Rheology and structure of mixtures formed by the polysaccharides waxy corn starch and gellan. México: Universidad Nacional Autónoma de México, PhD thesis.

Rodríguez-Hernández, A. I., Durand, S., Garnier, C., Tecante, A. and Doublier, J. L. 2006. Rheology-structure properties of waxy maize starch-gellan mixtures. Food Hydrocolloids 20(8): 1223-1230.

Savary, G., Handschin, S., Conde-Petit, B., Cayot, N. and Doublier, J. L. 2008. Structure of polysaccharide-starch composite gels by rheology and confocal laser scanning microscopy: Effect of the composition and of the preparation procedure. Food Hydrocolloids 22(4): 520-530.

Shevkani, K., Singh, N., Singh, S., Ahlawat, A. K. and Singh, A. M. 2011. Relationship between physicochemical and rheological properties of starches from Indian wheat lines. International Journal of Food Science and Technology 46(12): 2584-2590.

Singh, N., Singh, J., Kaur, L., Singh Sodhi, N. and Singh Gill, B. 2003. Morphological, thermal and rheological properties of starches from different botanical sources. Food Chemistry 81(2): 219-231.

Warren, F. J., Gidley, M. J. and Flanagan, B. M. 2016. Infrared spectroscopy as a tool to characterize starch ordered structure—A joint FTIR-ATR, NMR, XRD and DSC study. Carbohydrate Polymers 139: 35-42.

Xiong, J., Li, Q., Shi, Z. and Ye, J. 2017. Interactions between wheat starch and cellulose derivatives in short-term retrogradation: Rheology and FTIR study. Food Research International 100: 858-863.

Xu, N., Zhang, Y., Zhang, G. and Tan, B. 2021. Effects of insoluble dietary fiber and ferulic acid on rheological and thermal properties of rice starch. International Journal of Biological Macromolecules 193: 2260-2270.

Zhan, Q., Ye, X., Zhang, Y., Kong, X., Bao, J., Corke, H. and Sui, Z. 2020. Starch granule-associated proteins affect the physicochemical properties of rice starch. Food Hydrocolloids 101: 105504.